Neuroscience 235 (2013) 226–231

GREY MATTER DENSITY AND $GABA_A$ BINDING POTENTIAL SHOW A POSITIVE LINEAR RELATIONSHIP ACROSS CORTICAL REGIONS

N. W. DUNCAN, [a,b] **P. GRAVEL,** [c] **C. WIEBKING,** [a,d] **A. J. READER** [c] **AND G. NORTHOFF** [a]*

[a] *Mind, Brain Imaging and Neuroethics Research Unit, Institute of Mental Health Research, University of Ottawa, Ottawa, Canada*

[b] *Department of Biology, Carleton University, Ottawa, Canada*

[c] *McConnell Brain Imaging Centre, Montreal Neurological Institute, McGill University, Montreal, Canada*

[d] *Department of Biology, Freie Universität Berlin, Berlin, Germany*

Abstract—Voxel based morphometry (VBM) is a widely used technique for studying the structure of the brain. Direct comparisons between the results obtained using VBM and the underlying histology are limited, however. To circumvent the problems inherent in comparing VBM data *in vivo* with tissue samples that must generally be obtained post-mortem, we chose to consider $GABA_A$ receptors, measured using ^{18}F-flumazenil PET (18F-FMZ-PET), as non-invasive neural markers to be compared with VBM data. Consistent with previous cortical thickness findings, $GABA_A$ receptor binding potential (BP_{ND}) was found to correlate positively across regions with grey matter (GM) density. These findings confirm that there is a general positive relationship between MRI-based GM density measures and $GABA_A$ receptor BP_{ND} on a region-by-region basis (i.e., regions with more GM tend to also have higher BP_{ND}).

Key words: VBM, receptor density, benzodiazepine receptor, flumazenil, anatomical imaging, brain morphometry.

INTRODUCTION

Voxel-based morphometry (VBM) (Ashburner and Friston, 2000) is a widely used MRI technique for studying brain structure. It has been used in many different research contexts, including social neuroscience (Kanai et al., 2011), memory (Kanai and Rees, 2011), depression (Bora et al., 2011), and Alzheimer's disease (Ferreira et al., 2011). However, the relationship between VBM measures and actual neural structure has not been well defined.

One approach to linking VBM measures and the underlying histology would be to compare *in vivo* MRI scans with post-mortem histology. However, given the obvious practical issues involved in such an approach, a non-invasive measure of neural structure is required that can then be compared with VBM data. In this context it has been suggested that ^{18}F-flumazenil PET (Ryzhikov et al., 2005) (18F-FMZ-PET) could be utilised as an indicator for neuronal density and integrity (Heiss et al., 1998; Hammers et al., 2001; la Fougère et al., 2011). This technique allows the imaging of $GABA_A$ receptors *in vivo* in humans (Hammers et al., 2003; Salmi et al., 2008) as flumazenil binds to the benzodiazepine site on the $GABA_A$ receptor (Sigel, 2002). With the $GABA_A$ receptor found widely across the human cortex, playing a major role in neural inhibition, the inference can potentially be drawn between $GABA_A$ receptor density and the density of neurons.

Adapting this approach, la Fougère et al. (2011) compared cortical thickness, as obtained through the analysis of MRI images, with $GABA_A$ receptor density, finding a correlation between these measures across the regions studied. This suggests that the link between $GABA_A$ receptors and morphological measures is valid in the context of cortical thickness analyses. It is not clear, however, if these findings can be extended to VBM.

We thus compared $GABA_A$ receptor density and VBM measures to establish whether this approach can be applied to VBM also. It was hypothesised that receptor density would correlate with VBM measurements across cortical regions. As a second, exploratory, aim we also investigated whether grey matter (GM) measurements within individual regions of interest correlated with $GABA_A$ receptor density within the same region.

EXPERIMENTAL PROCEDURES

Participants

Twenty-five healthy subjects (10 female; mean age 22.67 years, range 18–32 years) underwent both PET and MRI scanning. PET (Montreal Neurological Institute, McGill) and MRI (Unité de neuroimagerie fonctionelle, Université de Montréal) scans took place on different days (mean time between scans = 2.44 days, range = 1–6 days). PET scan sessions began at either 11 am or 1 pm; MRI scans were made at approximately 3 pm. Subjects were screened for psychiatric or neurological disorders, recreational drug use, and depression, the latter using the Beck Depression Inventory-II with a cut-off of four (Beck et al., 1996). All subjects gave their written informed

*Corresponding author. Address: Mind, Brain Imaging and Neuroethics Research Unit, Institute of Mental Health Research, 1145 Carling Avenue, Ottawa, ON, Canada K1Z 7K4. Tel: +1-613-722-6521x6801; fax: +1-613-798-2982.
E-mail address: georg.northoff@theroyal.ca (G. Northoff).
Abbreviations: BP_{ND}, binding potential; CSF, cerebrospinal fluid; 18F-FMZ-PET, ^{18}F-flumazenil PET; GM, grey matter; WM, white matter; VBM, Voxel based morphometry.

0306-4522/12 $36.00 © 2013 IBRO. Published by Elsevier Ltd. All rights reserved.
http://dx.doi.org/10.1016/j.neuroscience.2012.12.075

consent and were compensated financially for their participation. Approval was obtained from the ethics committees of both McGill University and the Université de Montréal. Image analyses were carried out using the FSL suite of tools (Smith et al., 2004).

MRI

T1-weighted anatomical images were acquired on a 3T Siemens Trio scanner using a 16-channel headcoil (MPRAGE, resolution = $1 \times 1 \times 1\,mm^3$). Anatomical images were processed in accordance with the FSL-VBM pipeline (Ashburner and Friston, 2000), as follows: Anatomical images were brain extracted and segmented into GM, white matter (WM), and cerebrospinal fluid (CSF) partial volume images. The GM images were aligned with the MNI template using a non-linear registration and averaged across subjects to produce a study-specific template. A non-linear registration was then performed between the original GM images and this study-specific template. Finally, the registered partial volume images were modulated (to correct for local expansion or contraction) by dividing by the Jacobian of the warp field.

PET

^{18}F-FMZ-PET data were acquired using a Siemens ECAT HRRT PET scanner. ^{18}F-flumazenil was synthesised as previously described (Massaweh et al., 2009). Head movement was minimised with a head-restraining adhesive band. A 6-min transmission scan (^{137}C-point source) was first acquired for attenuation correction followed by an intravenous tracer injection (over 60 s) of 260.7 MBq (±21.24 SD) of ^{18}F-flumazenil. Subjects were instructed to close their eyes and remain awake.

List-mode data were acquired for a period of 60 min and then binned into a series of 26 sequential sets of fully 3D sinograms of increasing duration, ranging from 30 s to 5 min. PET data were reconstructed using a 3D OP-OSEM algorithm (10 iterations and 16 subsets) with correction for scatter, random coincidences, attenuation, decay, dead-time, and frame-based motion correction (Hudson and Larkin, 1994; Hong et al., 2007; Costes et al., 2009). The resulting images were composed of voxels of $1.22 \times 1.22 \times 1.22\,mm^3$ ($256 \times 256 \times 207$ voxels). $GABA_A$ binding potential (BP_{ND}) maps were then calculated according to the simplified reference tissue method, using the cerebral WM as the reference tissue region (Logan et al., 1996).

The following steps were adopted to minimise partial volume effects: WM and CSF maps (where each voxel has a value of between 0 and 1, representing the estimated proportion of that voxel that can be assigned to the relevant tissue type) were first each thresholded at a tissue proportion of 0.95 and used to produce binary masks. The masks were eroded by two voxels to ensure that only the tissue type of interest (and not GM) was covered, and the mean BP_{ND} within these WM and CSF regions calculated. The original, non-eroded, WM and CSF maps were then convolved with a 2.5-mm FWHM Gaussian kernel to simulate the scanner resolution and were multiplied by the mean BP_{ND} value for the appropriate tissue (WM or CSF). These WM and CSF BP_{ND} maps were then subtracted from the original BP_{ND} maps to give GM BP_{ND} images corrected for WM and CSF signal spill over. To further reduce partial volume effects the atlas ROIs were eroded to produce a separation between each one (see below). The BP_{ND} values obtained were broadly comparable to those obtained in other studies (Odano et al., 2009; la Fougère et al., 2011).

BP_{ND} images were aligned to the study GM template in a two-step process. Firstly, the GM map in anatomical space was convolved with a 2.5-mm FWHM kernel to produce a "simulated PET" image. BP_{ND} images were then linearly aligned to this image. This linear transform was then combined with the previously calculated non-linear anatomical-to-template warp to transfer the BP_{ND} images into the template space. Alignment between the BP_{ND} and GM images can be seen in Fig. 1.

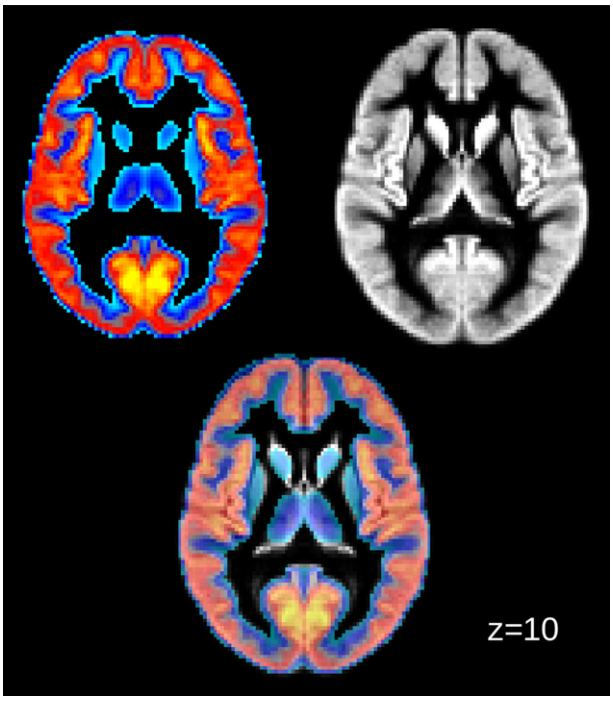

Fig. 1. Sample flumazenil BP_{ND} map and GM density image, plus the super-imposition of these to demonstrate alignment between modalities.

Regions of interest

Regions of interest were taken from the Jülich histological atlas (http://www.fmrib.ox.ac.uk/fsl/data/atlas-descriptions.html). This atlas consists of 52 GM regions (and 10 WM regions, not included here), bilaterally, and was created using post-mortem cyto-architectural segmentations. Following the creation of all 104 ROIs, the masks were eroded by one voxel in order to reduce partial volume effects, the voxel size (2 mm) corresponding reasonably well to the resolution of the PET scanner (FWHM approx 2.5 mm). This erosion also served to reduce the effects of misalignment at the borders of regions. Atlas ROIs were then masked with the study-specific brain template to ensure that no out-of-brain voxels were included in the calculations. ROIs consisting of fewer than 50 voxels after erosion were excluded from the analysis, leaving 59 out of 104 ROIs (see Table 1 for list of ROIs included).

The GM volume for each ROI from each subject was extracted from the registered GM maps. Mean BP_{ND} values were calculated for each ROI across subjects in the same manner.

Comparison of GM and BP_{ND}

Analyses of GM and BP_{ND} values were carried out using MATLAB 7.12 (The Mathworks, Natick, MA, USA). In the first step, mean BP_{ND} and GM values within each region (i.e., a mean value across subjects for each region was calculated and a single correlation done using regions as data-points) were compared using partial correlations, controlling for ROI size.

In an exploratory second step, the relationship between BP_{ND} and GM was then tested across subjects within each region independently (i.e., subject BP_{ND} and GM values were compared in 59 independent tests, one test per region, where

Table 1. ROIs used with ROI volume (voxels), and mean BP_{ND} and GM values (±SD). Also shown are *t*-statistics for the slope of the weighted linear fit between within-region BP_{ND} and GM. Amyg. = amygdala, Ant. IPS = anterior intra-parietal sulcus, Hippo. = hippocampus, IPL = inferior parietal lobule, 1° Motor = primary motor cortex, Premotor = premotor cortex, 1° SS = primary somatosensory cortex, 2° SS = secondary somatosensory cortex, SPL = superior parital lobule, V = visual cortex

	Left			Right			L	R
	Vol.	BP_{ND}	GM	Vol.	BP_{ND}	GM	BP_{ND} vs.	GM
Ant. IPS 1	125	5.64 ± 0.98	0.45 ± 0.08	84	5.36 ± 1.08	0.46 ± 0.12	1.57	2.72*
Ant. IPS 3	58	5.71 ± 1.11	0.34 ± 0.10	–	–	–	1.24	–
Broca's (BA44)	1480	7.71 ± 0.87	0.55 ± 0.08	853	8.37 ± 1.08	0.6 ± 0.08	0.11	0.07
Borca's (BA45)	1224	8.16 ± 1.05	0.60 ± 0.09	1148	7.38 ± 1.02	0.50 ± 0.07	0.97	0.16
IPL PF	367	8.66 ± 1.00	0.61 ± 0.10	328	8.05 ± 1.31	0.69 ± 0.1	−1.73*	−1.46
IPL PFcm	86	7.32 ± 0.76	0.61 ± 0.19	–	–	–	−1.17	–
IPL PFm	75	8.86 ± 1.04	0.61 ± 0.12	237	8.14 ± 0.95	0.66 ± 0.10	−0.89	−0.75
IPL Pga	164	8.42 ± 1.00	0.59 ± 0.11	433	8.34 ± 0.94	0.66 ± 0.10	0.66	−1.71*
IPL PGp	796	8.08 ± 0.98	0.59 ± 0.08	822	8.28 ± 0.99	0.60 ± 0.08	0.01	−0.16
Premotor	4285	7.19 ± 0.93	0.58 ± 0.07	4218	6.90 ± 0.87	0.55 ± 0.05	−0.51	−0.53
1° Motor	178	6.44 ± 0.91	0.49 ± 0.10	136	6.18 ± 0.91	0.43 ± 0.07	0.05	−0.49
1° SS (BA1)	175	6.89 ± 1.16	0.54 ± 0.09	133	5.46 ± 1.37	0.48 ± 0.08	0.28	−0.84
1° SS (BA2)	92	8.10 ± 1.02	0.50 ± 0.12	94	7.62 ± 1.19	0.54 ± 0.09	0.72	0.72
2° SS OP1	171	8.97 ± 1.02	0.64 ± 0.11	133	9.06 ± 1.20	0.65 ± 0.10	−1.55	0.36
2° SS OP3	121	7.51 ± 0.77	0.59 ± 0.08	140	7.00 ± 0.87	0.53 ± 0.07	−0.93	−1.21
2° SS OP4	183	7.82 ± 0.97	0.61 ± 0.11	156	6.50 ± 1.01	0.52 ± 0.11	−0.55	−1.01
SPL 5Ci	54	8.46 ± 1.17	0.60 ± 0.12	123	8.64 ± 1.06	0.59 ± 0.10	1.43	0.53
SPL 5L	65	6.78 ± 1.24	0.51 ± 0.11	97	5.93 ± 1.19	0.43 ± 0.12	0.36	−0.03
SPL 5M	110	9.11 ± 1.18	0.61 ± 0.09	56	8.05 ± 1.21	0.56 ± 0.12	−0.68	−1.42
SPL 7A	891	6.48 ± 0.90	0.48 ± 0.07	393	6.74 ± 0.87	0.51 ± 0.09	−0.94	−0.80
SPL 7M	–	–	–	70	9.06 ± 1.00	0.67 ± 0.11	–	1.68
SPL 7P	228	5.43 ± 1.02	0.41 ± 0.07	349	6.38 ± 0.99	0.49 ± 0.10	0.85	−1.10
V1	513	9.00 ± 1.19	0.48 ± 0.07	783	9.18 ± 1.18	0.54 ± 0.09	−0.45	1.23
V2	405	6.46 ± 0.92	0.46 ± 0.06	711	7.50 ± 0.83	0.56 ± 0.08	−0.32	1.38
V3	70	7.63 ± 0.90	0.62 ± 0.11	89	7.32 ± 1.03	0.62 ± 0.11	1.67	2.51*
V4	481	7.66 ± 0.82	0.68 ± 0.07	416	7.14 ± 0.92	0.71 ± 0.11	−0.38	0.67
V5	285	8.00 ± 0.82	0.62 ± 0.13	315	8.73 ± 1.10	0.62 ± 0.13	−0.24	0.93
Amyg. LBG	56	5.00 ± 0.85	0.73 ± 0.06	62	3.85 ± 0.56	0.51 ± 0.06	1.60	1.88*
Hippo. CA	111	6.00 ± 0.76	0.81 ± 0.09	134	4.15 ± 0.59	0.63 ± 0.08	1.71	2.48*
Hippo. EC	334	5.91 ± 0.73	0.71 ± 0.15	402	6.17 ± 0.66	0.82 ± 0.16	0.80	0.88
Hippo. Sub	90	3.90 ± 0.66	0.48 ± 0.10	112	3.70 ± 0.57	0.46 ± 0.08	2.63*	1.92*

* Indicates $p = 0.01$–0.05, not corrected for multiple comparisons).

each data-point represents a subject). Weighted least squares fits were employed to test for a linear relationship between the two measures, using the inverse variance of each particular ROI's BP_{ND} values (i.e., the variance of the values of all voxels within each ROI for each subject) as a weighting factor to account to some degree for PET measurement error.

The significance level for all tests was set at $p < 0.05$ following FDR correction for multiple comparisons, other than in the exploratory least squares fit analysis where an uncorrected $p < 0.05$ was used.

RESULTS

GM and BP values

Mean BP_{ND} values ranged from 3.7 in the right subiculum of the hippocampus to 9.18 in the right primary visual cortex. Mean GM ranged from 0.34 in the left anterior intra-parietal sulcus to 0.82 in the right entorhinal cortex. Details for all regions can be found in Table 1. No significant difference in mean BP_{ND} or mean GM values between hemispheres was observed (paired *t*-test, BP_{ND} $p_{FDR} = 0.57$, GM $p = 0.64$). There were no correlations between ROI size and mean BP ($r = 0.096$, $p_{FDR} = 0.45$, 95% CI = −0.16 to 0.39) or mean GM ($r = -0.06$, $p_{FDR} = 0.67$, 95% CI = −0.33 to 0.21).

Global BP_{ND}–GM correlation

Mean BP_{ND} and mean GM were positively correlated across regions ($r = 0.35$, $p_{FDR} = 0.012$, 95% CI = 0.11–0.56). Subsequent appraisal of the scatter-plot of the BP_{ND} and GM data suggested two distinct groupings of regional values (Fig. 2). The larger (51 ROIs) of these consisted of cortical regions, whilst the smaller (8 ROIs) consisted of subcortical regions (amygdala and hippocampus) (see Table 1). The distinction between the two groups was due to lower mean BP_{ND} values in the subcortical regions, consistent with prior findings of systematically lower $GABA_A$ receptor binding in such areas (Odano et al., 2009). Based on this cortical–subcortical distinction, separate correlations were carried out for each sub-group. In the larger, cortical, group, mean BP_{ND} and mean GM across regions were positively correlated ($r = 0.69$, $p_{FDR} < 0.0001$, 95% CI = 0.52–0.82). This was also the case in the smaller, subcortical, group ($r = 0.94$, $p_{FDR} = 0.018$, 95% CI = 0.69–0.99).

The positive correlation seen between BP_{ND} and GM is in contrast to that reported by la Fougère et al. (2011) between BP_{ND} and cortical thickness, where a negative correlation was found. To help clarify the difference in

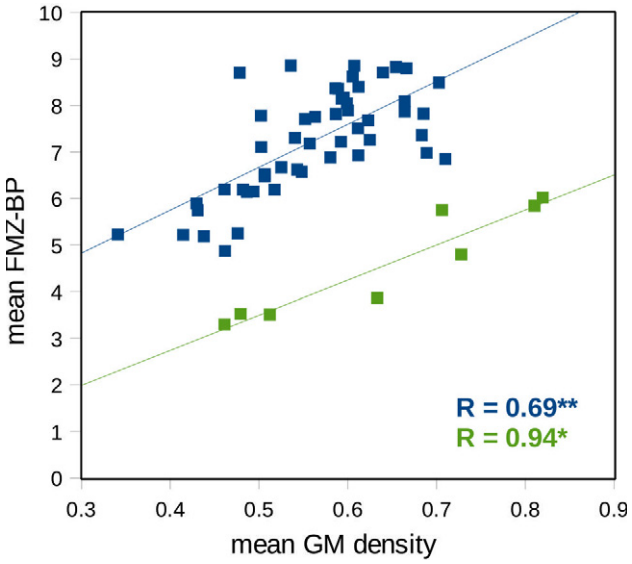

Fig. 2. Correlation between mean BP_{ND} and mean GM in each of the two identified groupings of ROIs. Blue points correspond to cortical regions (see Table 1 for full list of regions). Green points correspond to regions of the hippocampus and amygdala. * Denotes $p_{FDR} < 0.05$, ** denotes $p_{FDR} < 0.001$. All regions taken together were also positively correlated ($r = 0.35$, $p_{FDR} = 0.012$). (For interpretation of the references to colour in this figure legend, the reader is referred to the web version of this article.)

results, we carried out a supplementary analysis comparing BP_{ND} and cortical thickness in this group of participants. The standard Freesurfer pipeline was used to produce cortical thickness measurements (Fischl and Dale, 2000), with values then being extracted for each subject from each region from the whole-brain Harvard-Oxford atlas (http://www.cma.mgh.harvard.edu/fsl_atlas.html). This atlas was used in this analysis rather than the Jülich histological atlas in order to correspond more closely with the methodology employed by la Fougère et al. (2011), where a whole-brain atlas was employed. As with the GM analysis, ROIs with fewer than 50 voxels were excluded. Confirming previous results, a negative correlation was seen between BP_{ND} and cortical thickness ($r = -0.41$, $p_{FDR} = 0.0012$, 95% CI = −0.58 to −0.20).

Regional BP_{ND}–GM correlation

A positive correlation between BP_{ND} and GM was seen in regions of the right anterior intra-parietal sulcus, the right amygdala, bilateral hippocampus, and right V3 (uncorrected *p*-values). Whilst the majority of significant relationships were positive, some regions displayed a negative correlation between the two measures, including sections of the inferior parital lobule and secondary somatosensory cortex (see Table 1 for details). These results must be treated with great caution, however, as they are not significant following correction for multiple comparisons.

DISCUSSION

Using a combination of high-resolution ^{18}F-FMZ-PET and VBM, we investigated the relationship between $GABA_A$ receptor density and GM density in regions of the cortex defined according to a histological atlas. $GABA_A$ BP_{ND} was found to correlate with GM density on a region-by-region basis. This finding echoes previous findings that show a correlation between $GABA_A$ receptor density and cortical thickness across regions (la Fougère et al., 2011). The direction of the correlation is reversed in VBM as compared to cortical thickness, however, with a positive correlation compared to a negative one, respectively. To explain this we can consider the nature of the two measurements. VBM gives information as to the volume of GM that is present in a region (Ashburner and Friston, 2000): the positive correlation thus represents the relationship between the total volume of GM and the number of receptors to bind – with more GM there are more receptors. In contrast, and as discussed in la Fougère et al. (2011), cortical thickness could be described as giving a measure of the distribution of the GM within a region – with greater cortical thickness there is more space, so to speak, in which to distribute neurons and hence lower densities (although this will be variable across different regions Collins et al., 2010). With greater cortical thickness, and hence lower density, one would then expect a lower BP_{ND} value within a specific region. This can be illustrated by taking the primary visual cortex as an example: In the present study this region was found to have both a large GM density and high BP (see Table 1), whilst la la Fougère et al. (2011) observed high BP_{ND} but low cortical thickness (i.e., high GM density). This explanation is supported by our supplementary analysis which found, in agreement with la Fougère et al. (2011), a negative correlation between BP_{ND} and cortical thickness measures in the current sample.

Taking each of the Jülich atlas regions separately, a positive linear relationship between BP_{ND} and GM was seen in some regions, although the majority of regions showed no effect. A number of regions displayed a negative relationship (see Table 1). These correlations were not particularly significant, however, and did not remain following correction for multiple comparisons. As such they must be treated with caution. The conclusion that there is no correlation between BP_{ND} and GM within any particular region would be in agreement with the results of the one prior study directly comparing within-region VBM measures with histology (Eriksson et al., 2009). This study involved temporal lobe epilepsy patients undergoing surgical ablation of the seizure focus – the temporal lobe was scanned and a standard VBM analysis carried out before the anterior temporal lobe was then surgically removed and the neuronal density directly calculated. No correlation was found between MRI measures of GM and actual neuronal density, nor with a range of other histopathological measures. The apparent variability across regions of the relationship between regional ^{18}F-FMZ-PET and GM is also in accordance with the plasticity of the $GABA_A$ receptor (Arancibia-Carcamo and Kittler, 2009; Vithlani et al., 2011), as well as with prior work showing that the functional state of GABA-ergic neurons (i.e., the release

and uptake of the transmitter during activity) alters the affinity of the benzodiazepine site to which flumazenil binds (Miller et al., 1988; Frankle et al., 2012).

Some limitations of the current study must be considered. Firstly, PET and MRI scans were carried out on different days for practical reasons. As the retest reliability of binding potentials calculated using the simplified reference tissue approach adopted here is not ideal (Salmi et al., 2008) (although it should be noted that the data used in Salmi et al. were acquired using ^{11}C-flumazenil rather than ^{18}F-flumazenil), this may introduce some error into the measurements. Similarly, scans were not always taken at the same time of the day, which may also affect the results gained. Replication using data acquired more closely together and at the same time of day is thus required. Secondly, as the histological atlas used does not cover the whole brain, there may be differences in results when a segmentation of the entire cortex is used. An analysis of this dataset using the whole-brain Harvard–Oxford atlas (http://www.cma.mgh.harvard.edu/fsl_atlas.html) produced analogous results to those obtained with the Jülich atlas (inter-regional correlation, $R = 0.44$, $p < 0.0001$, 95% CI = 0.22–0.56); however, as there must be questions regarding the closeness of match between such regional atlases and the underlying cortical organisation (Craddock et al., 2011), the possibility must remain open that different results would be found with a whole-brain histological atlas. Thirdly, the menstrual cycle is known to affect GABA concentrations in different brain regions (Epperson et al., 2002; Harada et al., 2011), which may in turn affect $GABA_A$ receptor binding. Although the balance of males to females in this study may have served to reduce the impact of such an effect, further research into the effect of the menstrual cycle on $GABA_A$ receptors and their relationship to structural measures is required. Finally, as described above, the lack of correlation within individual regions may be due to the noise level in the data at the subject level being too high. The reasonable subject number ($n = 25$) and high-resolution data, coupled with the use of weighting to try and account for this factor, would suggest that this is not the case, but replication with a larger sample is warranted.

To conclude, using a combination of VBM and 18F-FMZ-PET it was shown that there is a general positive relationship between regional-mean $GABA_A$ BP_{ND} and regional-mean GM across histologically delineated regions of the brain. A more complex relationship of the within-region ^{18}F-FMZ-PET BP_{ND} values and GM at the single subject level was, however, suggested by there being only a weak linear relationship between the two measures in a minority of the regions studied.

Acknowledgements—The authors would like to thank K. Dedovic and A. Perna for their help with subject recruitment, as well the staff at the MNI for their assistance. Our thanks also to the anonymous reviewers for their constructive comments. The study was supported by Grants to G.N. (Canadian Institutes of Health Research (CIHR) and Hope for Depression Research Foundation (HDRF)).

REFERENCES

Arancibia-Carcamo I, Kittler J (2009) Regulation of GABA A receptor membrane trafficking and synaptic localization. Pharmacol Ther 123:17–31.

Ashburner J, Friston KJ (2000) Voxel-based morphometry – the methods. NeuroImage 11:805–821.

Beck AT, Steer RA, Ball R, Ranieri W (1996) Comparison of beck depression inventories -IA and -II in psychiatric outpatients. J Pers Assess 67:588–597.

Bora E, Fornito A, Pantelis C, Yücel M (2011) Gray matter abnormalities in major depressive disorder: a meta-analysis of voxel based morphometry studies. J Affect Disord. http://dx.doi.org/10.1016/j.jad.2011.03.049.

Collins CE, Airey DC, Young N, et al (2010) Neuron densities vary across and within cortical areas in primates. Proc Natl Acad Sci U S A 107:15927–15932. http://dx.doi.org/10.1073/pnas.1010356107.

Costes N, Dagher A, Larcher K, et al (2009) Motion correction of multi-frame PET data in neuroreceptor mapping: simulation based validation. Neuroimage 47:1496–1505.

Craddock RC, James GA, Holtzheimer PE, et al (2011) A whole brain fMRI atlas generated via spatially constrained spectral clustering. Hum Brain Mapp 1928:1914–1928. http://dx.doi.org/10.1002/hbm.21333.

Epperson CN, Haga K, Mason GF, et al (2002) Cortical gamma-aminobutyric acid levels across the menstrual cycle in healthy women and those with premenstrual dysphoric disorder: a proton magnetic resonance spectroscopy study. Arch Gen Psychiatry 59:851–858. http://dx.doi.org/10.1001/archpsyc.59.9.851.

Eriksson SH, Free SL, Thom M, et al (2009) Quantitative grey matter histological measures do not correlate with grey matter probability values from in vivo MRI in the temporal lobe. J Neurosci Methods 181:111–118. http://dx.doi.org/10.1016/j.jneumeth.2009.05.001.

Ferreira LK, Diniz BS, Forlenza OV, et al (2011) Neurostructural predictors of Alzheimer's disease: a meta-analysis of VBM studies. Neurobiol Aging 32:1733–1741. http://dx.doi.org/10.1016/j.neurobiolaging.2009.11.008.

Fischl B, Dale AM (2000) Measuring the thickness of the human cerebral cortex from magnetic resonance images. Proc Natl Acad Sci U S A 97:11050–11055.

la Fougère C, Grant S, Kostikov A, et al (2011) Where in-vivo imaging meets cytoarchitectonics: the relationship between cortical thickness and neuronal density measured with high-resolution [18F]flumazenil-PET. NeuroImage 56:951–960. http://dx.doi.org/10.1016/j.neuroimage.2010.11.015.

Frankle WG, Cho RY, Mason NS, et al (2012) [C]flumazenil binding is increased in a dose-dependent manner with tiagabine-induced elevations in GABA levels. PloS One 7:e32443. http://dx.doi.org/10.1371/journal.pone.0032443.

Hammers A, Koepp MJ, Richardson MP, et al (2001) Central benzodiazepine receptors in malformations of cortical development: a quantitative study. Brain 124:1555–1565.

Hammers A, Koepp MJ, Richardson MP, et al (2003) Grey and white matter flumazenil binding in neocortical epilepsy with normal MRI. A PET study of 44 patients. Brain 126:1300.

Harada M, Kubo H, Nose A, et al (2011) Measurement of variation in the human cerebral GABA level by in vivo MEGA-editing proton MR spectroscopy using a clinical 3T instrument and its dependence on brain region and the female menstrual cycle. Hum Brain Mapp 32:828–833. http://dx.doi.org/10.1002/hbm.21086.

Heiss W-D, Grond M, et al (1998) Permanent cortical damage detected by flumazenil positron emission tomography in acute stroke. Stroke 29:454–461. http://dx.doi.org/10.1161/01.STR.29.2.454.

Hong I, Chung S, Kim H, Kim Y (2007) Ultra fast symmetry and SIMD-based projection–backprojection (SSP) algorithm for 3-D PET image reconstruction. IEEE Trans Med Imaging 26:789–803. http://dx.doi.org/10.1109/TMI.2002.808360.

Hudson HM, Larkin RS (1994) Accelerated image reconstruction using ordered subsets of projection data. IEEE T Med Imaging 13:601–609.

Kanai R, Bahrami B, Roylance R, Rees G (2011) Online social network size is reflected in human brain structure. Proc R Soc B. http://dx.doi.org/10.1098/rspb.2011.1959.

Kanai R, Rees G (2011) The structural basis of inter-individual differences in human behaviour and cognition. Nat Rev Neurosci 12:231–242. http://dx.doi.org/10.1038/nrn3000.

Logan J, Fowler JS, Volkow ND, et al (1996) Distribution volume ratios without blood sampling from graphical analysis of PET data. J Cereb Blood Flow Metab 16:834–840.

Massaweh G, Schirrmacher E, la Fougere C, et al (2009) Improved work-up procedure for the production of [18F] flumazenil and first results of its use with a high-resolution research tomograph in human stroke. Nucl Med Biol 36:721–727.

Miller L, Greenblatt D, Barnhill J, et al (1988) ''GABA shift'' in vivo: enhancement of benzodiazepine binding in vivo by modulation of endogenous GABA. Eur J Pharmacol 148:123–130.

Odano I, Halldin C, Karlsson P, et al (2009) [18F]flumazenil binding to central benzodiazepine receptor studies by PET–quantitative analysis and comparisons with [11C]flumazenil. NeuroImage 45:891–902. http://dx.doi.org/10.1016/j.neuroimage.2008.12.005.

Ryzhikov N, Seneca N, Krasikova R (2005) Preparation of highly specific radioactivity flumazenil and its evaluation in cynomolgus monkey by positron emission tomography. Nucl Med Biol 32:109–116.

Salmi E, Aalto S, Hirvonen J, et al (2008) Measurement of GABAA receptor binding in vivo with [11C] flumazenil: a test–retest study in healthy subjects. Neuroimage 41:260–269.

Sigel E (2002) Mapping of the benzodiazepine recognition site on GABA-A receptors. Curr Top Med Chem 2:833–839.

Smith SM, Jenkinson M, Woolrich MW, et al (2004) Advances in functional and structural MR image analysis and implementation as FSL. Neuroimage 23:S208–S219.

Vithlani M, Terunuma M, Moss SJ (2011) The dynamic modulation of GABA(A) receptor trafficking and its role in regulating the plasticity of inhibitory synapses. Physiol Rev 91:1009–1022. http://dx.doi.org/10.1152/physrev.00015.2010.

(Accepted 18 December 2012)
(Available online 1 February 2013)